DOI: 10.1002/ejic.201000549

Orientation of Second-Harmonic-Generation-Active Phenylsulfonyl Chromophores Attached on Layered Lead(II) Phosphonates

Zi-Yi Du,*[a] Yu-Hui Sun,[a] Xiang Xu,[b] Guo-Hai Xu,[a] and Yong-Rong Xie*[a]

Keywords: Lead / Phosphonates / Crystal growth / Nonlinear optics

The hydrothermal reactions of $PbCl_2$ or $PbBr_2$ with diethyl [(phenylsulfonyl)methyl]phosphonate afforded two lead(II) phosphonates with the formula $[Pb_3(Ph–SO_2–CH_2–PO_3)_2X_2(H_2O)]$ [X = Cl (**1**) and Br (**2**)]. The two compounds are isostructural and exhibit a lamellar structure in which the phenylsulfonyl chromophores orient unilaterally on the inorganic layer of $[Pb_3(PO_3)_2X_2(H_2O)]$. The acentric stacking of such layers results in their crystallization in the noncentrosymmetric *Cc* space group, and both compounds show second harmonic generation responses comparable to that of KDP (KH_2PO_4).

Introduction

Over the past a few decades, second-order nonlinear optical (NLO) materials have attracted significant attention owing to their pivotal role in the domain of photoelectronics and photonics.[1] In recent years, with the development of crystal engineering, various metal-organic frameworks exhibiting a second-order NLO effect have also been explored.[2] The development of such molecule-based, second-order NLO materials is usually realized through two major steps. The first is the synthesis of a second-order NLO chromophore possessing a large hyperpolarizability (β) and the second involves the assembly of these molecular building blocks into a noncentrosymmetric bulk structure with a suitable orientation of the β tensor components. Whereas the first level of molecular synthesis has been widely explored, both theoretically and experimentally,[3] the organization of these chromophores into optimal lattice structures with the desired molecular orientations is still a difficult problem.

It is well known that metal phosphonates are useful for organizing molecules into lamellar structures in which the metal ions are bridged by the phosphonate moieties to form an inorganic layer; the remaining organic group of the phosphonate generally dangles in the interlayer region.[4] Based on this prominent characteristic, metal phosphonates (especially zirconium phosphonates) have been widely used for the assembly of second-order NLO chromophores into noncentrosymmetric multilayer films.[5] Inspired by this "layer-by-layer" approach, we deem that a similar strategy is also realizable through the crystal engineering technique, i.e., the growing of noncentrosymmetric layered metal phosphonates with second-harmonic-generation-(SHG)-active chromophores oriented in the interlayer region, as depicted in Scheme 1. Although a few SHG-active metal phosphonate crystals have been isolated,[6,7] to date the orientation of the SHG-active chromophores attached on layered metal phosphonate crystals has not been reported.

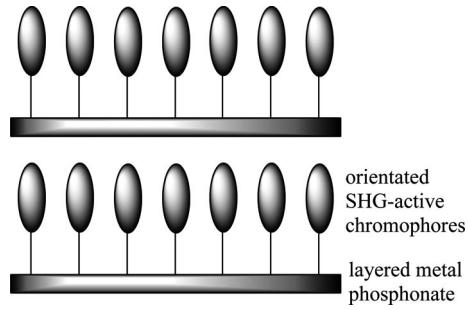

Scheme 1. Orientation of SHG active chromophores on layered metal phosphonate.

In this context, we use a ligand in which a phosphonate moiety is directly combined with a SHG-active phenylsulfonyl chromophore, i.e., $Ph–SO_2–CH_2–PO_3H_2$ (H_2L), as a building block to address the above issue. Our research efforts yielded two such layered lead(II) phosphonates with the formula $[Pb_3(L)_2X_2(H_2O)]$ [X = Cl (**1**) and Br (**2**)]. Herein, we report their syntheses, X-ray structures, and second-order NLO properties.

[a] College of Chemistry and Life Science, Gannan Normal University,
Ganzhou, 341000, P. R. China
[b] State Key Laboratory of Structural Chemistry, Fujian Institute of Research on the Structure of Matter, Chinese Academy of Sciences,
Fuzhou, 350002, P. R. China
E-mail: ziyidu@gmail.com
yongrongxie@163.com

Supporting information for this article is available on the WWW under http://dx.doi.org/10.1002/ejic.201000549.

Results and Discussion

Synthesis

The preparation of compounds **1** and **2** relies on the well-established hydrothermal method using diethyl phosphonate as starting material. During the course of the hydrothermal treatment, the high temperature and high pressure aid the hydrolysis of the phosphonic ester to produce phosphonic acid in situ (Scheme 2). It is believed that the slow, in situ formation of phosphonic acid facilitates the growth of single crystals.[8] It was also observed that the addition of a small amount of acid to the aqueous solution helped improve the crystalline quality of the two compounds.

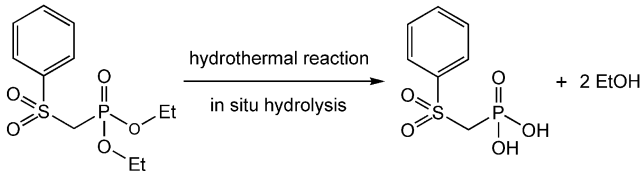

Scheme 2. The in situ hydrolysis of the diethylphosphonate ester.

Crystal Structure Description

Compounds **1** and **2** are isostructural, hence only the structure of **1** will be discussed in detail. Compound **1** crystallizes in the monoclinic *Cc* space group and features a novel 2D-layered structure. The asymmetric unit contains three unique Pb^{2+} ions with coordination numbers ranging from four to six (Figure 1), all of which featured a hemidirected geometry, using the terminology of Glusker et al.[9] The Pb1 ion is six-coordinate with four phosphonate O atoms from three L^{2-} anions and two chloride anions, the Pb2 ion is five-coordinate with three phosphonate O atoms and one sulfone O atom from three L^{2-} anions as well as one chloride anion, whereas the Pb3 ion is four-coordinate with two phosphonate O atoms from two L^{2-} anions and one chloride anion as well as an aqua ligand. Their coordination geometry can be described as a distorted ψ-PbO_4Cl_2 pentagonal bipyramid, a severely distorted ψ-PbO_4Cl octahedron, and a severely distorted ψ-PbO_3Cl trigonal bipyramid, respectively. Each ion has one site occupied by a lone electron pair. The Pb–O [2.286(8)–2.757(8) Å] and Pb–Cl [2.633(4)–3.080(4) Å] distances are comparable to those reported for other lead(II) phosphonates.[10]

There are two unique L^{2-} anions, two unique Cl^- anions, and one unique H_2O molecule serving as ligands in compound **1**. As shown in Figure 1, the two L^{2-} ligands in **1** adopt two types of coordination modes and can be written as $[4.2_{12}1_31_41_30]$ (for the ligand containing the P1 and S1 atoms, denoated L_A) and $[4.2_{12}2_{13}1_400]$ (for the ligand containing the P2 and S2 atoms, denoted L_B) according to the Harris notation.[11] Both ligands have pentadentate coordination and bridge three Pb^{2+} ions and chelate a fourth. There is, however, one bidentate and two monodentate phosphonate O atoms and one monodentate sulfone O atom in L_A, whereas there are two bidentate and one monodentate phosphonate O atoms in L_B. The two chelating atoms in L_A contain one monodentate phosphonate O atom and one monodentate sulfone O atom, whereas those in L_B contain two bidentate phosphonate O atoms. The interconnection of the Pb^{2+} ions by the above two types of L^{2-} ligands leads to the formation of a complicated 2D-layered structure; the spare coordination sites of the Pb^{2+} ions are filled by bidentate Cl^- ligands and monodentate aqua ligands (Figure 2).

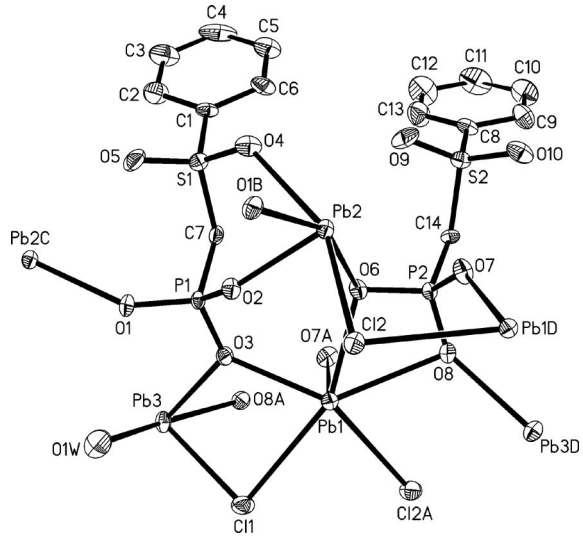

Figure 1. The ORTEP representation of the selected unit of **1**. The thermal ellipsoids are drawn at 30% probability. Symmetry codes for the generated atoms: A. *x*, –*y* + 1, *z* – 1/2; B. *x*, –*y*, *z* + 1/2; C. *x*, –*y*, *z* – 1/2; D. *x*, –*y* + 1, *z* + 1/2.

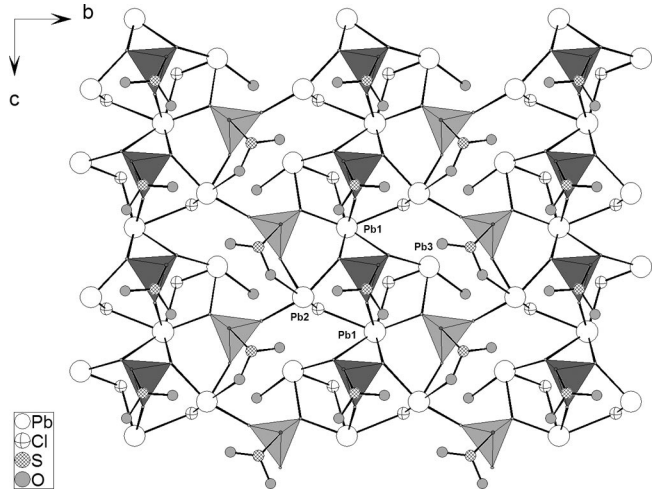

Figure 2. View of the layered structure of **1** down the *a* axis. The $CP1O_3$ and $CP2O_3$ tetrahedra are shaded in light and medium grey, respectively. Phenyl groups of the L^{2-} ligands have been omitted for clarity.

The layered structure of **1** features a distinctive 1D $\{[Pb_3(L_B)Cl_2(H_2O)]^{2+}\}_n$ cationic chain along the *c* axis, which contains a cyclic Pb_4 unit with neighboring Pb_4 units linked together in a corner-shared fashion. The intercon-

nection of these 1D $\{[Pb_3(L_B)Cl_2(H_2O)]^{2+}\}_n$ chains through the L_A ligands constitutes the extended 2D-layered architecture along the *bc*-plane. Specifically, the phenylsulfonyl chromophores attached on the phosphonate ligands orient unilaterally on the 2D layer, and as such noncentrosymmetric 2D layers stack along the *a* axis by van der Waals forces with adjacent layers related only by translational symmetry along the *b* axis (Figure 3). Consequently, compound **1** crystallizes in the noncentrosymmetric *Cc* space group.

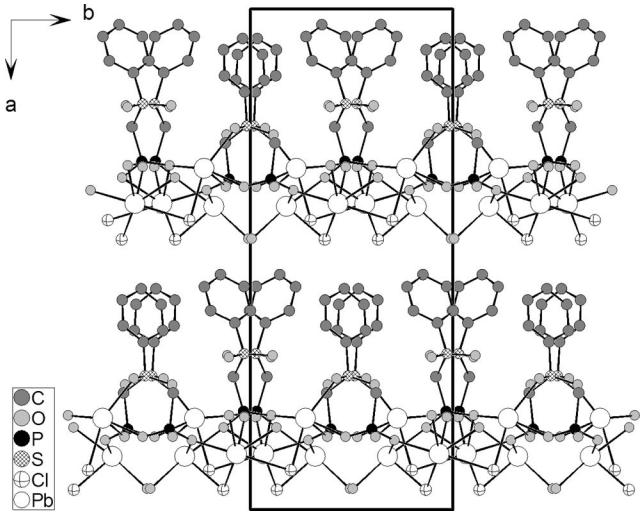

Figure 3. View of the structure of **1** down the *c* axis.

Compound **2** has a similar structure to **1**. The main difference being the Cl^- ligands in **1** are replaced by Br^- ligands in **2**. As a result, the unit cell volume of **2** [2610.19(8) Å^3 is slightly larger than that of **1** [2532.62 (13) Å^3], owing to the longer Pb–Br distances [2.7772(19)–3.245(2) Å] in **2** compared with the Pb–Cl distances [2.633(4)–3.080(4) Å] in **1**.

Nonlinear Optical Properties

In view of the fact that both compounds crystallize in a noncentrosymmetric space group (*Cc*), we investigated the SHG measurements[12] on sieved powdered samples of **1** and **2**. The preliminary experimental results indicated that both **1** and **2** are NLO-active and exhibit SHG efficiencies of ≈ 1 and 2 times that of KDP, respectively. Furthermore, both compounds were found to be phase-matchable (Figures S1 and S2 in the Supporting Information). The SHG efficiency can be mainly attributed to the orderly arrangement of the SHG-active phenylsulfonyl chromophores. In addition, the SHG efficiency of **2** is somewhat larger than that of **1**, presumably because the electron-withdrawing ability of the chloride anion is stronger than that of the bromide.[13]

Thermogravametric Analysis

The Thermogravametric analysis (TGA) curve of **1** exhibits two main weight loss steps (Figure S3 in the Supporting Information). The first step, completed at 172 °C, corresponds to the release of one water molecule. The observed weight loss of 1.5% is equal to the calculated value. The second step started at 365 °C and ended at 440 °C and corresponds to the decomposition of the ligands. The total weight loss at 750 °C is 30.3%; the final residues were not characterized. The TGA curve of **2** shows three main weight loss steps. The first step, as for **1**, corresponds to the loss of water; the dehydrated material was then stable up to 365 °C. The second and the third steps, however, are overlapping and weight loss continues until 750 °C, corresponding to the decomposition of the ligands. The total weight loss at 750 °C is 36.8%; the final residues were not characterized.

Conclusion

In summary, by the hydrothermal reaction of $PbCl_2$ or $PbBr_2$ with diethyl [(phenylsulfonyl)methyl]phosphonate, two lead(II) phosphonates $[Pb_3(Ph–SO_2–CH_2–PO_3)_2X_2(H_2O)]$ [X = Cl (**1**) and Br (**2**)] were obtained. The two compounds are isostructural and exhibit a lamellar structure in which the phenylsulfonyl chromophores orient unilaterally on the inorganic layer of $[Pb_3(PO_3)_2X_2(H_2O)]$. The present work serves as a nice example in which second-order NLO materials can be rationally designed based on layered metal phosphonates. Further research will be extended to investigate other second-order NLO materials based on layered metal phosphonates.

Experimental Section

Materials and Instrumentation: Diethyl [(phenylsulfonyl)methyl]-phosphonate ($Ph–SO_2–CH_2–PO(OEt)_2$) was synthesized using a published procedure.[14] All other chemicals were obtained from commercial sources and used without further purification. Elemental analyses were performed on a German Elementary Vario EL III instrument. FT-IR spectra were recorded on a Nicolet 5700 spectrometer using KBr pellets in the range of 4000–400 cm^{-1}. X-ray powder diffraction (XRD) patterns (Cu-K_α) were collected on a Bruker Advance D8 θ–2θ diffractometer. Thermogravimetric analyses were carried out on a Diamond TG/DTA 6000 unit at a heating rate of 15 °C/min under a nitrogen atmosphere. The measurements of the powder frequency-doubling effects were carried out by the method of Kurtz and Perry.[12] Radiation of 1064 nm was generated by a Q-switched Nd: YAG solid-state laser was used as the fundamental frequency light. The crystal sample was ground and sieved into several distinct particle sizes (25–45, 45–53, 53–75, 75–105, 105–150, 150–210 μm for **1**; 45–53, 53–75, 75–105, 105–150, 150–210, 210–300 μm for **2**). The samples of known particle sizes were packed into round glass boxes with a uniform diameter of 8.0 mm and then exposed to laser radiation. The second harmonic radiation generated by the randomly oriented microcrystals was detected by a photomultiplier tube and displayed on an oscilloscope. Samples of KDP were prepared as reference materials in identical fashion to assume the SHG effect.

Synthesis of $[Pb_3(L)_2Cl_2(H_2O)]$ (1): A mixture of $PbCl_2$ (0.32 mmol), $Ph–SO_2–CH_2–PO(OEt)_2$ (0.30 mmol), and two drops of an HCl solution (1 M) in distilled water (12 mL) was sealed in a

Parr Teflon-lined autoclave (23 mL) and heated at 150 °C for 3 d. The final pH value was ≈ 2.0 and colorless plate-shaped crystals of **1** were collected in approximately 78% yield (0.098 g) based on Pb. The purity was confirmed by powder XRD (Figure S4 in the Supporting Information). $C_{14}H_{16}Cl_2O_{11}P_2Pb_3S_2$ (1178.80): calcd. C 14.26, H 1.37; found C 14.21, H 1.45. IR (KBr): $\tilde{\nu}$ = 3441(s), 3064(m), 2979(m), 2920(m), 2362(m), 1631(m), 1476(m), 1443(m), 1379(m), 1298(s), 1269(s), 1207(m), 1182(s), 1144(vs), 1116(s), 1077(s), 1029(s), 981(s), 797(m), 759(m), 728(m), 684(m), 614(m), 545(m), 494(m), 467(m) cm^{-1}.

Synthesis of $[Pb_3(L)_2Br_2(H_2O)]$ (2): A mixture of $PbBr_2$ (0.32 mmol), $Ph–SO_2–CH_2–PO(OEt)_2$ (0.30 mmol) and two drops of an HNO_3 solution (1 M) in distilled water (12 mL) was sealed in a Parr Teflon-lined autoclave (23 mL) and heated at 150 °C for 3 d. The final pH value was ≈ 2.0 and colorless plate-shaped crystals of **2** were collected in a approximately 75% yield (0.101 g) based on Pb. The purity was confirmed by powder XRD (Figure S5 in the Supporting Information). $C_{14}H_{16}Br_2O_{11}P_2Pb_3S_2$ (1267.72): calcd. C 13.26, H 1.27; found C 13.19, H 1.36. IR (KBr): $\tilde{\nu}$ = 3436 (s), 3058 (m), 2978 (m), 2919 (m), 2362 (m), 1621 (m), 1586 (m), 1478 (m), 1445 (m), 1377 (m), 1297 (s), 1271 (s), 1207 (m), 1184 (s), 1144 (vs), 1118 (s), 1078 (s), 1025 (s), 978 (s), 795 (m), 759 (m), 728 (m), 683 (m), 613 (m), 545 (m), 493 (m), 469 (m) cm^{-1}.

Single-Crystal Structure Determination: Data collection for compounds **1** and **2** was performed on a Smart ApexII CCD diffractometer equipped with a graphite-monochromated Mo-K_α radiation (λ = 0.71073 Å). Intensity data for both compounds were collected using ϕ and ω scans at 296 K. The data sets were corrected for Lorentz and polarization factors, as well as for absorption by using the SADABS program.[15] Both structures were solved by the direct method and refined by full-matrix least-squares fitting on F^2 by SHELX-97.[16] All non-hydrogen atoms were refined with anisotropic thermal parameters. All hydrogen atoms were generated geometrically and refined isotropically. The hydrogen atoms for the water molecules are not included in the refinements. It is worth noting that both compounds were analysed as a racemic crystal structure in the polar space group *Cc*, although the analysed crystals of both were found to be twinned by inversion, with the Flack parameter being 0.667(19) and 0.51(2), respectively. Crystallographic data and structural refinements for **1** and **2** are summarized in Table 1, relevant bond lengths are listed in Table 2.

Table 1. Summary of crystal data and structural refinements for compounds **1** and **2**.

	1	**2**
Empirical formula	$C_{14}H_{16}O_{11}P_2S_2Cl_2Pb_3$	$C_{14}H_{16}O_{11}P_2S_2Br_2Pb_3$
Formula weight	1178.80	1267.72
Space group	*Cc*	*Cc*
a [Å]	25.0502(7)	25.5867(4)
b [Å]	10.1591(3)	10.2311(2)
c [Å]	9.9560(3)	9.9756(2)
α [deg]	90	90
β [deg]	91.656(2)	91.7520(10)
γ [deg]	90	90
V [$Å^3$]	2532.62(13)	2610.19(8)
Z	4	4
D_{calcd} [$g\,cm^{-3}$]	3.092	3.226
μ [mm^{-1}]	20.448	22.698
GOF on F^2	1.010	0.984
R_1, wR_2 [$I > 2\sigma(I)$][a]	0.0238, 0.0488	0.0276, 0.0510
R_1, wR_2 (all data)	0.0269, 0.0497	0.0331, 0.0525

[a] $R_1 = \Sigma||F_o| - |F_c||/\Sigma|F_o|$, $wR_2 = \{\Sigma w[(F_o)^2 - (F_c)^2]^2/\Sigma w[(F_o)^2]^2\}^{1/2}$.

Table 2. Selected bond lengths [Å] for compounds **1** and **2**.[a]

1			
Pb(1)–O(7)#1	2.286(8)	Pb(1)–O(3)	2.470(8)
Pb(1)–O(6)	2.491(9)	Pb(1)–O(8)	2.757(8)
Pb(1)–Cl(2)#1	3.052(3)	Pb(1)–Cl(1)	3.080(4)
Pb(2)–O(2)	2.347(8)	Pb(2)–O(1)#2	2.464(8)
Pb(2)–O(6)	2.526(7)	Pb(2)–O(4)	2.727(9)
Pb(2)–Cl(2)	2.740(3)	Pb(3)–O(3)	2.449(8)
Pb(3)–O(8)#1	2.456(8)	Pb(3)–Cl(1)	2.633(4)
Pb(3)–O(1 W)	2.689(10)		
2			
Pb(1)–O(7)#1	2.302(10)	Pb(1)–O(3)	2.470(9)
Pb(1)–O(6)	2.472(10)	Pb(1)–O(8)	2.752(10)
Pb(1)–Br(2)#1	3.2013(17)	Pb(1)–Br(1)	3.245(2)
Pb(2)–O(2)	2.334(9)	Pb(2)–O(1)#2	2.455(9)
Pb(2)–O(6)	2.520(9)	Pb(2)–O(4)	2.731(11)
Pb(2)–Br(2)	2.8862(18)	Pb(3)–O(3)	2.439(10)
Pb(3)–O(8)#1	2.456(9)	Pb(3)–O(1 W)	2.648(13)
Pb(3)–Br(1)	2.7772(19)		

[a] Symmetry codes for both compounds: #1 x, $-y + 1$, z -2; #2 x, $-y$, $z + 1/2$.

CCDC-776499 (for **1**) and 776500 (for **2**) contain the supplementary crystallographic data for this paper. These data can be obtained free of charge from The Cambridge Crystallographic Data Centre via www.ccdc.cam.ac.uk/data_request/cif.

Supporting Information (see footnote on the first page of this article): Phase matching curves for **1** and **2** (Figures S1, S2); TGA curves for **1** and **2** (Figure S3); simulated and experimental XRD powder patterns for **1** and **2** (Figures S4, S5).

Acknowledgments

This work was supported by the National Natural Science Foundation of China (Grant 20861001), the Natural Science Foundation of Jiangxi Province (Grant 2008GQH0013), the Natural Science Foundation of Jiangxi Provincial Education Department (Grant GJJ09317), and the Key Laboratory of Jiangxi University for Functional Materials Chemistry.

[1] a) B. E. A. Saleh, M. C. Teich, *Fundamentals of Photonics*, Wiley, New York, **1991**; b) J. Zyss (Ed.), *Molecular Nonlinear Optics: Materials, Physics and Devices*, Academic Press, New York, **1994**.

[2] a) O. R. Evans, W. Lin, *Acc. Chem. Res.* **2002**, *35*, 511–522; b) S. Jayanty, P. Gangopadhyay, T. P. Radhakrishnan, *J. Mater. Chem.* **2002**, *12*, 2792–2797; c) M. J. Prakash, T. P. Radhakrishnan, *Inorg. Chem.* **2006**, *45*, 9758–9764; d) Z. Guo, R. Cao, X. Wang, H. Li, W. Yuan, G. Wang, H. Wu, J. Li, *J. Am. Chem. Soc.* **2009**, *131*, 6894–6895.

[3] a) J. Zyss, I. Ledoux, *Chem. Rev.* **1994**, *94*, 77–105; b) D. R. Kanis, M. A. Ratner, T. J. Marks, *Chem. Rev.* **1994**, *94*, 195–242; c) T. J. Marks, M. A. Ratner, *Angew. Chem. Int. Ed. Engl.* **1995**, *34*, 155–173.

[4] a) G. Cao, H.-G. Hong, T. E. Mallouk, *Acc. Chem. Res.* **1992**, *25*, 420–427; b) A. Clearfield, *Metal Phosphonate Chemistry*, in: *Progress in Inorganic Chemistry* (Ed.: K. D. Karlin), vol. 47, John Wiley & Sons, New York, **1998**, p. 371–510; c) K. Maeda, *Microporous Mesoporous Mater.* **2004**, *73*, 47–55; d) G. K. H. Shimizu, R. Vaidhyanathan, J. M. Taylor, *Chem. Soc. Rev.* **2009**, *38*, 1430–1449.

[5] a) H. E. Katz, G. Scheller, T. M. Putvinski, M. L. Schilling, W. L. Wilson, C. E. D. Chidsey, *Science* **1991**, *254*, 1485–1487; b) G. A. Neff, M. R. Helfrich, M. C. Clifton, C. J. Page, *Chem.*

Mater. **2000**, *12*, 2363–2371; c) S. B. Bakiamoh, G. J. Blanchard, *Langmuir* **2001**, *17*, 3438–3446; d) T. Morotti, V. Calabrese, M. Cavazzini, D. Pedron, M. Cozzuol, A. Licciardello, N. Tuccitto, S. Quici, *Dalton Trans.* **2008**, 2974–2982.
[6] P. Ayyappan, O. R. Evans, Y. Cui, K. A. Wheeler, W. Lin, *Inorg. Chem.* **2002**, *41*, 4978–4980.
[7] X.-G. Liu, K. Zhou, J. Dong, C.-J. Zhu, S.-S. Bao, L.-M. Zheng, *Inorg. Chem.* **2009**, *48*, 1901–1905.
[8] a) G. B. Hix, B. M. Kariuki, M. Tremayne, *Inorg. Chem.* **2001**, *40*, 1477–1481; b) X.-M. Zhang, *Coord. Chem. Rev.* **2005**, *249*, 1201–1219; c) Z.-Y. Du, H.-R. Wen, Y.-R. Xie, *J. Mol. Struct.* **2008**, *891*, 272–277.
[9] L. Shimoni-Livny, J. P. Glusker, C. P. Bock, *Inorg. Chem.* **1998**, *37*, 1853–1867.
[10] a) B.-P. Yang, J.-G. Mao, Y.-Q. Sun, H.-H. Zhao, A. Clearfield, *Eur. J. Inorg. Chem.* **2003**, 4211–4217; b) Z.-M. Sun, J.-G. Mao, Y.-Q. Sun, H.-Y. Zeng, A. Clearfield, *New J. Chem.* **2003**, *27*, 1326–1330.
[11] R. A. Coxall, S. G. Harris, D. K. Henderson, S. Parsons, P. A. Tasker, R. E. P. Winpenny, *J. Chem. Soc., Dalton Trans.* **2000**, 2349–2356.
[12] S. W. Kurtz, T. T. Perry, *J. Appl. Phys.* **1968**, *39*, 3798–3813.
[13] Y.-T. Wang, G.-M. Tang, Y.-Q. Wei, T.-X. Qin, T.-D. Li, C. He, J.-B. Ling, X.-F. Long, S. W. Ng, *Cryst. Growth Des.* **2010**, *10*, 25–28.
[14] D. Enders, S. von Berg, B. Jandeleit, *Org. Synth.* **2002**, *78*, 169.
[15] *APEX2*, *SADABS* and *SAINT*, Bruker AXS Inc., Madison, Wisconsin, USA, **2008**.
[16] G. M. Sheldrick, *Acta Crystallogr., Sect. A* **2008**, *64*, 112–122.

Received: May 17, 2010
Published Online: September 7, 2010

